ISSN 1027-4510, Journal of Surface Investigation: X-ray, Synchrotron and Neutron Techniques, 2022, Vol. 16, No. 1, pp. 33–41. © Pleiades Publishing, Ltd., 2022.
Russian Text © The Author(s), 2022, published in Poverkhnost', 2022, No. 1, pp. 41–50.

Influence of Pulsed Flows of Deuterium Ions and Deuterium Plasma on Cu–Ni and Cu–Ni–Ga Alloys

V. N. Pimenov[a, *], I. V. Borovitskaya[a, **], V. A. Gribkov[a], A. S. Demin[a], N. A. Epifanov[a, b], S. A. Maslyaev[a], E. V. Morozov[a], I. P. Sasinovskaya[a], G. G. Bondarenko[b, c], A. I. Gaydar[c], and M. Paduch[d]

[a] *Baikov Institute of Metallurgy and Materials Science, Russian Academy of Sciences, Moscow, 119334 Russia*
[b] *National Research University Higher School of Economics, Moscow, 101000, Russia*
[c] *Scientific Research Institute of Advanced Materials and Technologies, Moscow, 115054 Russia*
[d] *Institute of Plasma Physics and Laser Microfusion, Warsaw, 01-497, Poland*
**e-mail:pimval@mail.ru*
***e-mail: symp@imet.ac.ru*

Received June 28, 2021; revised July 25, 2021; accepted July 30, 2021

Abstract—Experiments on the irradiation of Cu–4 wt % Ni and Cu–4 wt % Ni–10 wt % Ga copper alloys by high-power pulsed flows of deuterium plasma and deuterium ions are carried out in the Plasma Focus PF-1000 installation. The alloys are irradiated in two modes: the hard mode of combined action of deuterium plasma flows at $q_{pl} = 10^8–10^9$ W/cm^2, $\tau_{pl} = 100$ ns and deuterium ions at $q_i = 10^9–10^{10}$ W/cm^2, $\tau_i = 50$ ns and also in more soft conditions: the Cu–4 wt % Ni alloy is irradiated with a deuterium plasma flow at a power density of $q_i = 2 \times 10^7$ W/cm^2 and pulse duration of $\tau_{pl} = 100$ ns; the Cu–4 wt % Ni–10 wt % Ga alloy, at $q_{pl} = 5 \times 10^7–10^8$ W/cm^2 and $q_i = 10^8–10^9$ W/cm^2 and the same values of the pulse duration. The nature of the damage for Cu–4 wt % Ni and Cu–4 wt % Ni–10 wt % Ga alloys in the irradiation modes implemented is approximately the same and is determined by the wavy surface relief, the presence of craters, micropores, droplet-like fragments, and the absence of microcracks. Unlike the Cu–4 wt % Ni alloy, the surface structure of the Cu–4 wt % Ni–10 wt % Ga copper alloys has, after irradiation, a cellular or cellular–dendritic character. The parameters of the formation of such a structure depend on the regime of pulsed irradiation of the sample target and the conditions of subsequent directed crystallization of the molten surface layer. The formation of this structure is also significantly affected by alloying of the binary copper–nickel alloy with a third element (gallium) and probably the dendritic structure of the alloy in the initial state of the alloys. Plastic deformation is observed in the surface layer of each of the studied alloys after exposure to the flows of deuterium plasma and deuterium ions, which proceed by the sliding mechanism along the planes of the densest packing {111}, typical of materials with a face-centered cubic (fcc) lattice. The ductile copper Cu–Ni and Cu–Ni–Ga alloys under study, as well as the Cu–10 wt % Ga alloy studied previously, exhibit very high crack resistance to the effects of high-power pulsed radiation-thermal loads generated in a Plasma Focus PF-1000 installation, as compared to the refractory metals W, Mo, and V.

Keywords: pulsed flows, deuterium plasma, deuterium ions, plasma-focus device, damage, crystallization, cellular structure, plastic deformation

DOI: 10.1134/S1027451022010153

INTRODUCTION

It is known that the treatment of materials by high-power pulsed energy flows using plasma installations, i.e., high-current accelerators of ion and electron beams, can be carried out under conditions, at which radiation, thermal, and shock-wave loads act simultaneously on a sample target [1–4]. Such complex treatment can lead, on the one hand, to a damage of a material (sometimes to its fracture) and, on the other hand, favor a change in the structure–phase state in irradiated surface layers and the formation of modified crystalline structures with new properties [5–8].

In this context, copper and copper-based alloys are widely used in various fields of science and engineering, and they are interesting for studying the influence on them of various types of pulsed radiation to improve the physical-mechanical and technological properties and also to estimate and predict their resistance to pulsed radiation-thermal and shock-wave loads. The abovementioned high-power pulsed shock loads act, partially, on materials of the internal sur-

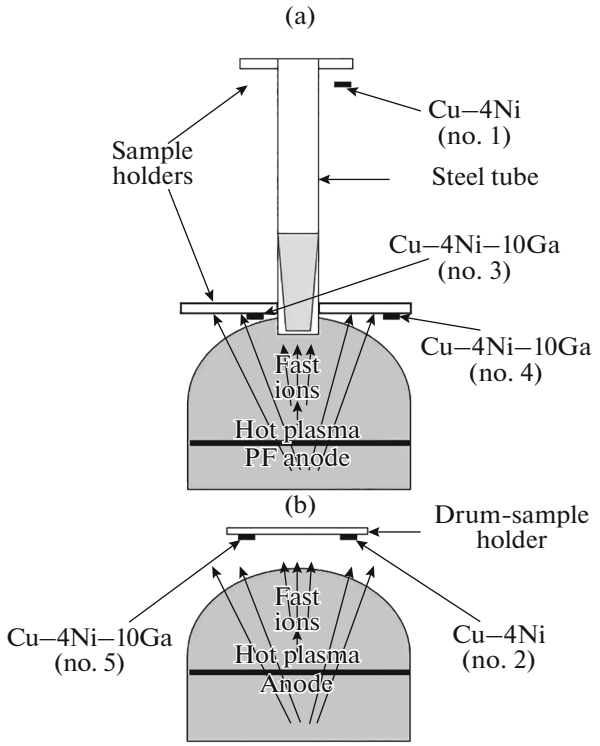

Fig. 1. Scheme of irradiation of Cu–4% Ni and Cu–4%Ni–4% Ga alloys in the Plasma Focus PF-1000 installation using (a) a hexahedral tube and (b) a drum for fixing the sample holders.

faces of chambers (first-wall materials) in thermonuclear-fusion installations with inertial confinement [9]. In this context, the behavior of ductile copper alloys under similar conditions are of a doubtless interest.

In publications, considerable attention is given to studies of the dependence of the surface state, the defect structure, and the elemental composition of the surface layer of copper–nickel foils on the parameters of irradiation with argon and boron ions in combination with their implantation [10–12]. Of increased interest is also the problem of the action of high-power ion beams [5, 13], pulsed laser radiation [14, 15], and shock waves [16–18] on copper and other alloys. The influence of complex radiation–thermal and shock-wave effects on copper and a copper–gallium alloy was studied in [19] using a Plasma Focus PF-1000 installation.

This work continues the studies performed in [19] and is devoted to studying the damage and deformation effects in surface layers of Cu–Ni and Cu–Ni–Ga alloys under acrtion on them of power pulse flows of deuterium plasma and deuterium ions generated in the Plasma Focus. PF-1000 setup.

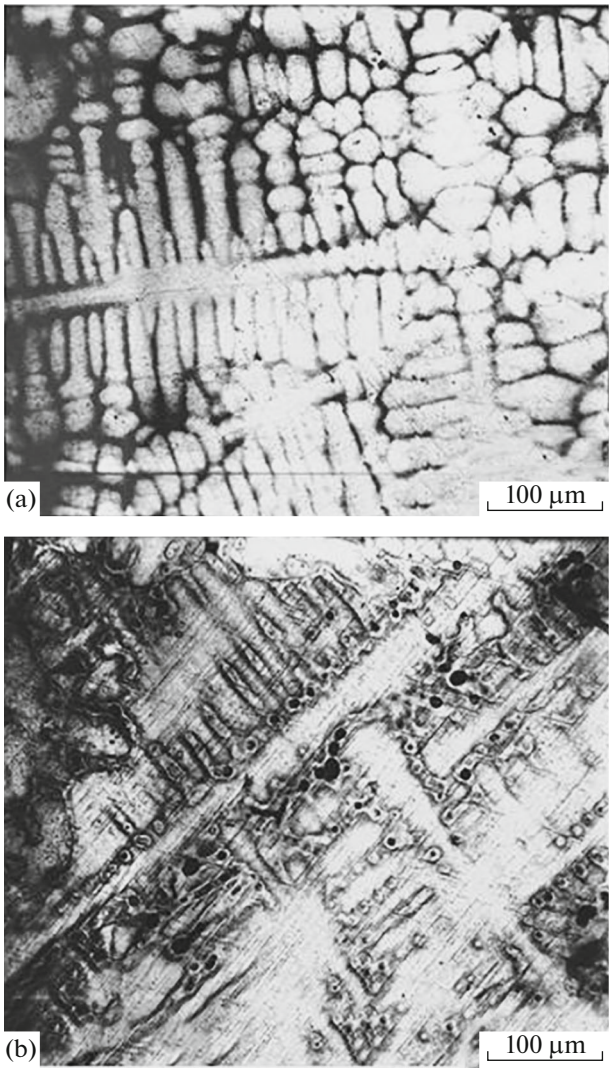

Fig. 2. Microstructure of fragments of (a) Cu–4% Ni and (b) Cu–4% Ni–4% Ga alloys in the initial state after melting (OM).

EXPERIMENTAL

Figure 1 shows the scheme of irradiating the samples using a Plasma Focus PF-1000 installation.

We studied Cu–4% Ni and Cu–4% Ni–10% Ga alloys (hereinafter, the contents are given in wt %), which were melted in an SShVL-16 vacuum furnace in graphite crucibles in the form of cylindrical samples with diameter $D = 9$ mm. After melting the alloys had a dendritic structure (Fig. 2) and were solid solutions of nickel in copper and nickel with gallium in copper, which were stable in a wide temperature range: from room temperature to the melting temperature. The alloys were cut into samples in the form of 2-mm-thick tablets. The experiments on irradiation using the Plasma Focus PF-1000 installation were carried out at an energy content 600 kJ. The working gas in the

Table 1. Parameters of irradiation of samples of Cu–4% Ni and Cu–4% Ni–10% Ga alloys with flows of deuterium plasma (DP) and deuterium ions (DI) in the Plasma Focus PF-1000 installation

Alloy composition and No. of sample	Distance from anode L, cm	DP flow density, W/cm^2	DP pulse duration τ, s	DI flow density, W/cm^2	DP pulse duration τ, s	Number of pulses N
	Experiment no. 1					
Cu–4Ni (no. 1)	40	2×10^7	10^{-7}	–	–	4
Cu–4Ni–10Ga (no. 3)	15	10^8	10^{-7}	10^8–10^9	5×10^{-8}	4
Cu–4Ni–10Ga (no. 4)	15	5×10^7	10^{-7}	10^8	5×10^{-8}	4
	Experiment no. 2					
Cu–4Ni (no. 2) Cu–4Ni–10Ga (no. 5)	12	10^8–10^9	10^{-7}	10^9 –10^{10}	5×10^{-8}	5

experiments was deuterium at an initial pressure in the chamber of $P = 470$ Pa. We used two irradiation techniques (Fig. 1), which were tested in [19] and allowed us to vary the condition of sample treatment with flows of deuterium plasma and deuterium ions with the energy of $E_i \geq 100$ keV. The Cu–4% Ni alloy was irradiated in two modes. In the case when the sample of this alloy was fixed at the back end of a hexahedral tube fabricated from 10Cr12G20V steel (Fig. 1a), only deuterium plasma acted on the sample, since the tube wall screened the sample from the flow of high-energy deuterium ions. In this case, the distance to the installation anode was $L = 40$ cm. On the other hand, as the samples of this alloy and Cu–4% Ni–10% Ga is arranged on the drum-holder wall fabricated of Cr18N9T steel (Fig. 1b), both flows of deuterium ions and deuterium plasma simultaneously act on each of the samples. The samples were at a distance of $L =$ 12 cm from the plasma-focus anode and were shifted by 5 cm from the chamber axis (Fig. 1b). Because in this case the angle of the expansion cone of fast ions generated in the plasma focus is 40 deg, the most powerful component of the ion beam, whose solid angle of divergence was 7–10 deg, did not act on the sample. This fact decreases the energy impact on the alloys and also decreases the flow power density by almost one order of magnitude, and no shock waves form in the volumes of the irradiated alloys. The simultaneous beam–plasma irradiation of Cu–4% Ni–10% Ga alloy was also carried out in the experiments when the samples of this alloy were fastened near the forward tube end at the distance $L = 15$ cm from the installation anode. In all these experiments, the sample targets were arranged in the cathode region of the plasma-focus chamber.

Table 1 gives the parameters of sample irradiation, where the experiments using a hexahedral tube are called "Experiment no. 1" and those using the drum holder, "Experiment no. 2".

The irradiated samples were studied by optical microscopy (OM) using a Neophot microscope and scanning electron microscopy (SEM) using a Zeiss EVO 40 scanning electron microscope with an adapter for local electron-probe X-ray microanalysis (EPMA).

RESULTS AND DISCUSSION

Damage of Copper Alloys

Figures 3 and 4 show the microstructures of the surfaces of the Cu–4% Ni alloy samples after their irradiation with pulsed flows of deuterium plasma

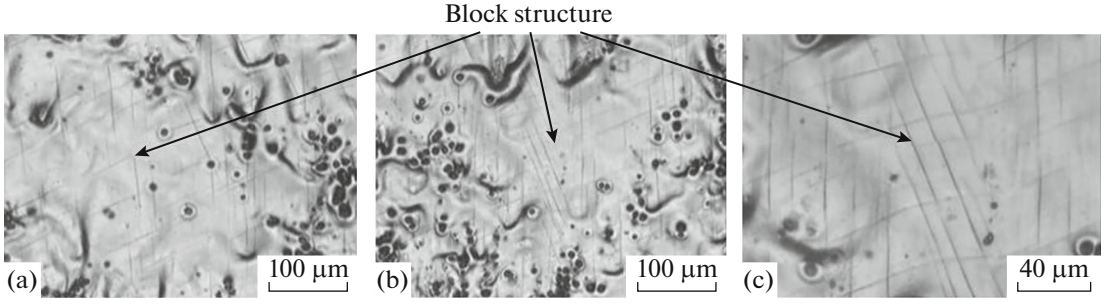

Fig. 3. Microstructure of fragments of the surface of the Cu–4% Ni alloy sample after irradiation in the Plasma Focus installation during experiment no. 1: distance from the anode $L = 40$ cm, $q_{pl} = 2 \times 10^7$ W/cm^2, $\tau = 100$ ns, the number of pulses $N = 4$ (OM).

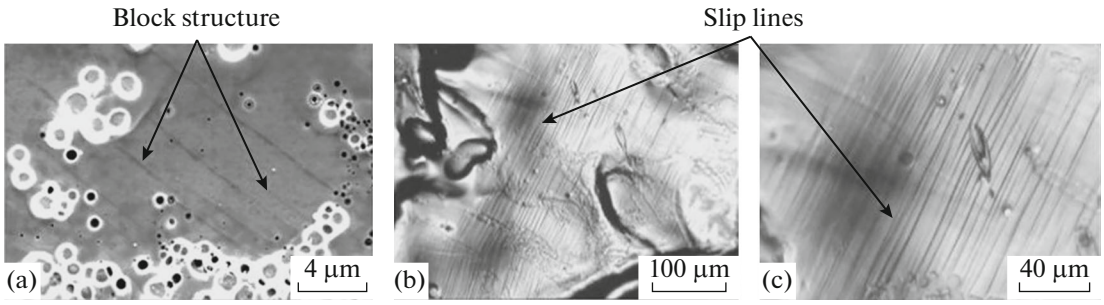

Fig. 4. Microstructure of fragments of the surface of the Cu–4% Ni–10% Ga alloy after irradiation in the Plasma Focus installation (Table 1): during experiment no. 1, sample 3 ($q_{pl} = 10^8$–10^9 W/cm^2, $\tau = 100$ ns, $q_i = 10^9$–10^{10} W/cm^2, $\tau = 50$ ns, the number of pulses $N = 5$: (a) SEM, (b, c) OM.

(Table 1, experiment no. 1) and simultaneous irradiation of flows of deuterium plasma and deuterium ions (Table 1, experiment no. 2). In both cases, the damage of the surface layer is typical, realized in metallic materials under similar conditions of plasma-beam irradiation [20–22]: on the irradiated surface, we see a wavy relief, craters, micropores, and droplet-like fragments, but there are no microcracks there. In the hardest conditions of irradiation (Table 1, exp. no. 2), the processes of erosion and removal of a surface layer part are due to an increase in material evaporation.

Figure 5 shows the character of damages of the Cu–4% Ni–10% Ga alloy at various irradiation modes. As seen from Fig. 1a, sample no. 3 of the alloy (Table 1) could be subjected to the action of flows of deuterium plasma and, partially, high-energy deuterium ions and underwent marked damage of the surface layer. The irradiated alloy surface (Fig. 5a) has a wavy character, contains many swells, pores, droplet-like deposits, and craters with a larger scatter of characteristic sizes from units and tens to several hundred micrometers. Such a surface shape shows that each of the energy-flow pulses causes explosive boiling accompanied by the processes of evaporation, erosion, formation of the liquid phase and rapid solidification in the surface layer.

The decrease in the energy-flow density acting on the surface layer of sample no. 4 as compared to sample no. 3 (Table 1) led to a decrease in its damage (Fig. 5b), which is demonstrated by a more smoothed relief, and also a decrease in the number of craters and their maximum sizes (from several hundred in sample No. 3 to several tens in sample no. 4 (Table 1)). In other words, the intensity of gas-phase exit from the melt with the formation of craters on its surface in sample no. 4 was lower than that in sample no. 3 (Table 1), which favored a decrease in the sizes and the amount. The existence of a gas phase in the molten surface layer is related to the existence of oxygen impurity in the initial state of the alloy and also to the implantation of deuterium ions into the material. Their capture by pores and vacancy complexes [23] with subsequent coagulation into microbubbles and their removal from the liquid phase, and also the possibility of the formation of the vapor phase due to the interaction of deuterium ions with the oxygen impurity presented in the alloy, favored the formation of the craters observed on the surface.

The Cu–4% Ni–10% Ga alloy sample fixed on the drum holder were irradiated in the hardest irradiation mode (Table 1). The damage of this alloy (Fig. 5a) was determined by a high intensity of erosion of the material, whose result is the removal of a noticeable part of the surface layer from the irradiated surface. Thus, the wavy surface of the alloy contains, after irradiation, a markedly smaller number of droplet-like fragments, craters, and pores as compared to the analogous alloy after experiments no. 1.

It should be emphasized in particular that all modes of thermal-radiation treatment do not lead to the formation of microcracks on the irradiated surface of Cu–4% Ni–10% Ga alloy, as well as Cu–4% Ni alloy. At the same time, the same and close conditions of plasma-beam impact on refractory materials (W, Mo, V, et al.) lead to the formation of microcracks in the irradiated surface layers [24–26].

Cellular Microstructure in the Cu–4% Ni–10% Ga Alloy

Our studies showed that the space between craters on the irradiated surface of the Cu–4% Ni–10% Ga alloy is a cellular microstructure, the cells have a droplet-like shape and their mean size is ~0.5–1 μm. Figure 6a shows a similar structure for sample no. 3 of the Cu–4% Ni–10% Ga alloy. It is interesting that, in some portions of the irradiated surface layer, some part of the cells is arranged along slip lines (Figs. 6b, 6c) which are formed due to plastic deformation of the material. In other portions, the cells are distributed homogeneously over the area occupied by them. In the hardest conditions of irradiation of Cu–4% Ni–

10% Ga alloy by flows of deuterium plasma and deuterium ions used in experiment no. 2 (Table 1), we observed dendrites on the irradiated surface (Fig. 7).

The existence of a cellular structure shows that the flat solidification front of the melt, which usually occurs upon the emergence of concentration supercooling ahead of the interface between the solid and liquid phases [27–29]. The cells on the irradiated alloy surface which have a droplet-like shape are the tops of columnar crystals, which were formed and grown during the process of directed crystallization of the surface-layer melt under conditions of concentration supercooling. It can be assumed that the branches of dendrites entering into the initial alloy structure (Fig. 2), which remained in the solid state in the surface layer under melt, contacted the liquid phase and became the centers of nucleation and subsequent fast growth of columnar crystals in the temperature-gradient direction.

We note that the formation of the columnar structure was observed in modified surface layers of various steels and nickel alloys after their irradiation with high-temperature pulsed plasma at $q_{pl} \geq 2 \times 10^6$ W/cm^2, τ = 3–50 μm [1] and also in tungsten under the action of deuterium plasma with a thermal load of 0.2–5 MJ/m^2 and pulse duration of 0.1–1.2 mc [30].

Particular attention is placed on the fact that no cellular structure formed in the surface layer of the binary Cu–4% Ni alloy after its irradiation with flows of deuterium plasma and deuterium ions. A similar situation took place in the Cu–10% alloy studied before [19] after plasma-beam irradiation approximately in the same mode. Cellular and cellular–dendritic structures (Figs. 6, 7) are observed in the ternary Cu–4% Ni–10% Ga alloy irradiated in conditions at which Cu–4% Ni alloy was irradiated (Table 1, experiment no. 2). Based on the obtained results, we can conclude that the increase in the doping levels of binary Cu–Ni and Cu–Ga alloys by adding the third component leads to the fact that, during solidification of the surface layer melted by pulsed irradiation, the flat solidification front loses its stability, supposedly, due to the appearance of the effect of concentration supercooling in the liquid solution. This was the reason for the formation of the abovementioned cellular and dendritic structures (Figs. 6, 7).

The influence of the concentration of doping elements on the morphological stability of the solidification front and the structural perfection of single crystals of nickel alloys was also observed in [31, 32].

Plastic Deformation in the Surface Layer

The irradiated surfaces of the alloys under study have marks of plastic deformation, i.e., slip lines.

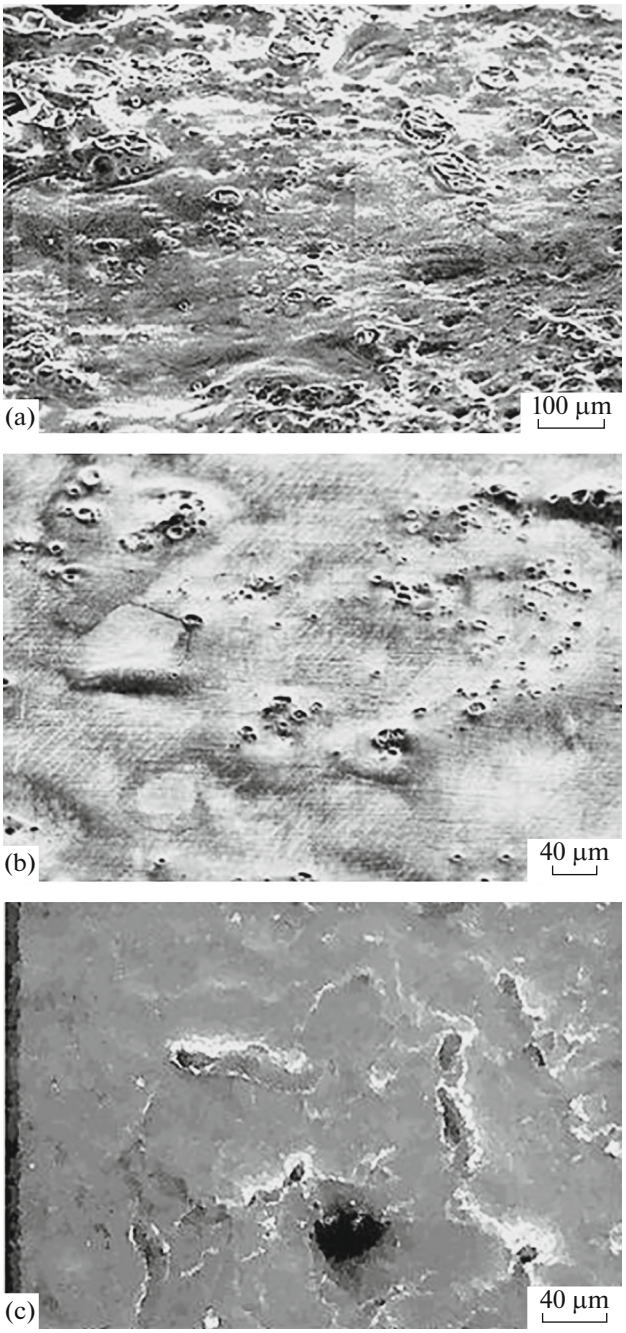

Fig. 5. Microstructure of fragments of the surface of the Cu–4% Ni–10% Ga alloy sample after irradiation in the Plasma Focus installation (Table 1): (a) experiment no. 3 ($q_{pl} = 10^8$–10^9 W/cm^2, $\tau = 100$ ns, $q_i = 10^9$–10^{10} W/cm^2, τ = 50 ns, the number of pulses $N = 4$); (b) experiment no. 1, sample 4 ($q_{pl} = 5 \times 10^7$ W/cm^2, $\tau = 100$ ns, $q_i = 10^8$–10^9 W/cm^2, $\tau = 50$ ns, the number of pulses $N = 4$); (c) experiment no. 2, sample 5 ($q_{pl} = 5 \times 10^7$ W/cm^2, $\tau = 100$ ns, $q_i = 10^8$ W/cm^2, $\tau = 50$ ns, N=4); в – exp. № 2, sample № 5 ($q_{pl} = 10^8$–10^9 W/cm^2, $\tau = 100$ ns, $q_i = 10^9$–10^{10} W/cm^2, $\tau = 50$ ns, the number of pulses $N = 5$ (SEM).

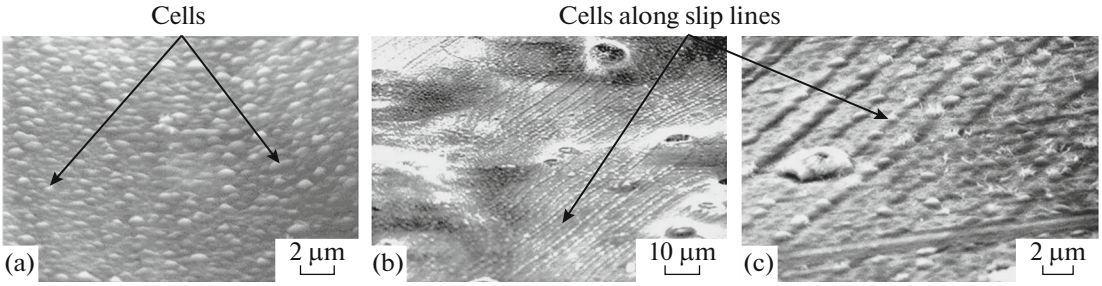

Fig. 6. Microstructure of fragments of the surface of sample 3 of the Cu–4% Ni–10% Ga alloy after irradiation in the Plasma Focus installation (Table 1) in experiment no. 1: $q_{pl} = 10^8$ W/cm^2, $\tau = 100$ nc, $q_i = 10^8$–10^9 W/cm^2, $\tau = 50$ ns, the number of pulses $N = 4$ (SEM).

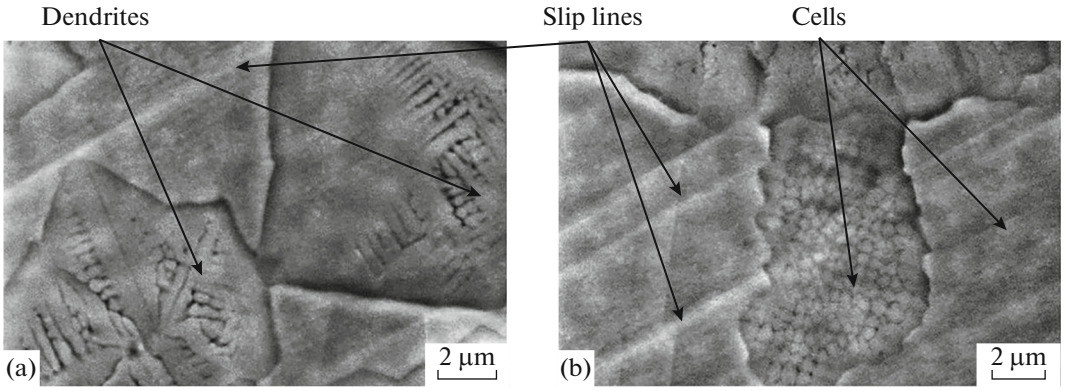

Fig. 7. Microstructure of fragments of the surface of sample 5 of the Cu–4% Ni–10% Ga alloy (Table 1) after irradiation in the Plasma Focus installation (Table 1) in experiment no. 2: $q_{pl} = 10^8$–10^9 W/cm^2, $\tau = 100$ ns, $q_i = 10^9$–10^{10} W/cm^2, $\tau = 50$ ns, the number of pulses $N = 5$ (SEM).

There are two types of slip lines in various portions of surface layers of the Cu–4% Ni: with the formation of block (Figs. 3 and 4a) and banded (Figs. 4b, 4c) microstructures. The character of plastic deformation in the Cu–4% Ni–10% Ga alloy (exp. 1, sample 4, Table 1) near the boundary of two grains is shown in Fig. 8. In one case (Fig. 8a), there is one system of slip lines which in the neighboring grains are arranged at an angle to each other; in another case (Fig. 8b), there are two systems of slip lines in each of the grains. Analysis shows, as a whole, that the main irradiation area of the alloy contains a "network" consisting of two systems of slip lines (Figs. 9a, 9b), and there are portions, in which there are three systems of slip lines (Fig. 9c).

The results obtained in this work allow us to conclude that plastic deformation in the surface layers of the irradiated samples of the Cu–4% Ni and Cu–4%Ni–10% Ga alloys proceeds by the mechanism of slipping over the densest packing planes {111} typical of fcc materials [23, 33]. This mechanism acted when the copper–nickel alloy was irradiated by deuterium plasma flows only (Fig. 3) and also during the simultaneous irradiation of each of the alloys by flows of deuterium plasma and deuterium ions (Figs. 4, 6–9). The existence of the block and banded microstructures indicates that plastic deformation in various local portions of the alloy surface took place using various slip systems permissible in fcc metals depending on the orientation of crystallites in these regions with respect to the axis of applied stress. The thermal stresses in the irradiated surface layers appeared at the stage of cooling the alloy samples after their irradiation with pulsed flows of deuterium plasma and deuterium ions. As a result of possible inhomogeneous distribution of the energy density over the ion-beam cross section during pulsed discharges in the plasma focus and, correspondingly, temperature fluctuations in the irradiated samples, the thermal stresses could be different in different microvolumes of the surface layers. In combination with different orientations of microcrystallites, the plastic deformation in local portions of surface layers of the alloys proceeded by the mechanism of slipping over planes {111} using the slip systems, which were preferential for the given region of irradiated alloys.

It should be noted that the irradiation mode, which is harder than that used in this work, combines high-power radiation–thermal action with shock-wave loads, and was used for irradiation of the solid solution of Cu–10% Ga in [19], can favor the plastic deformation process by the twinning mechanism [16–18].

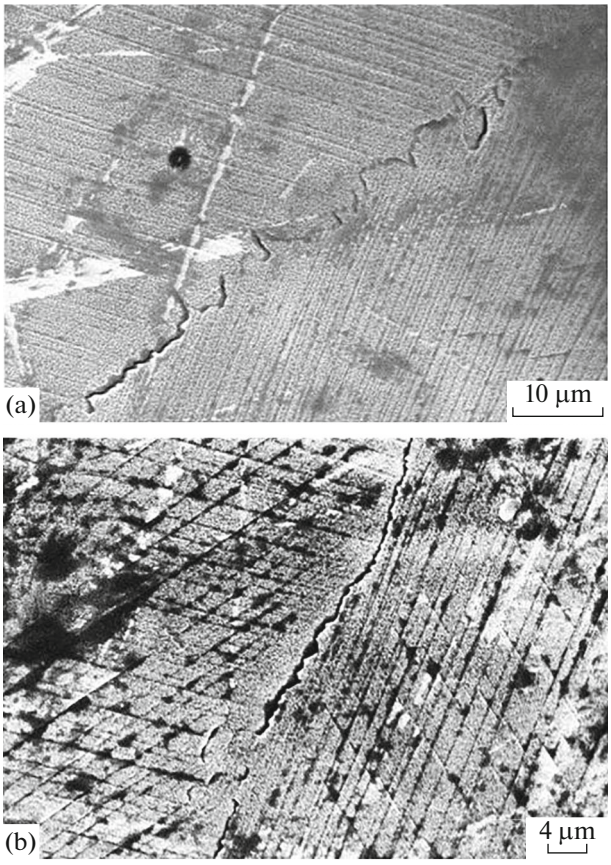

Fig. 8. Microstructure of fragments of the surface of sample 4 of the Cu–4% Ni–10% Ga alloy (Table 1) after irradiation in the Plasma Focus installation (Table 1) in experiment no. 1: $q_{pl} = 5 \times 10^7$ W/cm^2, $\tau = 100$ ns, $q_i = 10^8$ W/cm^2, $\tau = 50$ ns, the number of pulses $N = 4$ (SEM).

Elemental Analysis in the Surface Layer

Figure 10 shows the results of the X-ray spectral analysis of samples 4 and 5 of the Cu–4% Ni–10% Ga alloy after experiments carried out in this work. The analysis shows that the surface layer of the irradiated alloy contains, in addition to the main initial components, impurities of carbon, oxygen, and aluminum. Carbon and aluminum could be deposited on the sample–target surface after evaporation from the walls of functional materials of the plasma-focus chamber by high-power flows of deuterium plasma and deuterium ions. In this case, microparticles evaporated by the cluster mechanism under the action of flows of deuterium plasma and deuterium ions on the material of the sample holders also deposited onto the irradiated surface (Fig. 1). These microparticles also contained, alongside the elements noted above, the elements of the steel, from which the holders were made (Fig. 10b).

CONCLUSIONS

Experiments on the irradiation of Cu–4 wt % Ni and Cu–4 wt % Ni–10 wt % Ga copper alloys by high-power pulsed flows of deuterium plasma and deuterium ions have been carried out in the Plasma Focus installation. The alloys were irradiated in two modes: the hard mode of combined action of flows of deuterium plasma at $q_{pl} = 10^8$–10^9 W/cm^2, $\tau_{pl} = 100$ ns and deuterium ions at $q_i = 10^9$ –10^{10} W/cm^2, $\tau_i = 50$ ns and also softer conditions: the Cu–4 wt % Ni alloy was irradiated with the deuterium-plasma flow at a power density of $q_{pl} = 2 \times 10^7$ W/cm^2 and pulse duration of $\tau_{pl} = 100$ ns; the Cu–4 wt % Ni–10 wt % Ga alloy, at $q_{pl} = 5 \times 10^7$–10^8 W/cm^2 and $q_i = 10^8$–10^9 W/cm^2 and the same values of the pulse duration.

It is shown that the nature of the damage for Cu–4 wt % Ni and Cu–4 wt % Ni–10 wt % Ga alloys in the irradiation modes implemented is approximately the same and is determined by the wavy surface relief, the presence of craters, micropores, droplet-like fragments, and the absence of microcracks. Each energy-flow pulse acting on the alloy causes melting of its surface layer, explosive boiling with the formation of craters and pores, and also evaporation of the material (erosion process). In the harder irradiation mode, the processes noted above were amplified and accompanied by the removal of a part of the surface layer due to material erosion.

Unlike the Cu–4% Ni alloy, the structure of the surface layers of the Cu–4% Ni–10% Ga alloy in the used irradiation modes after their melting by plasma-beam irradiation and solidification of the liquid phase is of the cellular or cellular–dendritic type. The

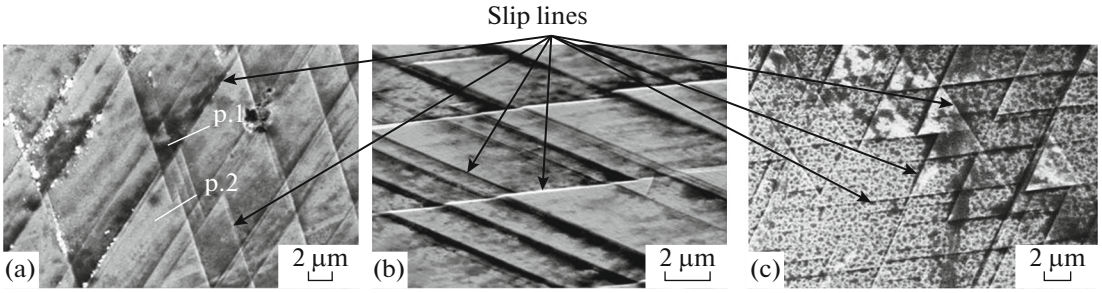

Fig. 9. Microstructure of fragments of the surface of sample 4 of the Cu–4% Ni–10% Ga alloy (Table 1) after irradiation in the Plasma Focus installation in experiment no. 1.

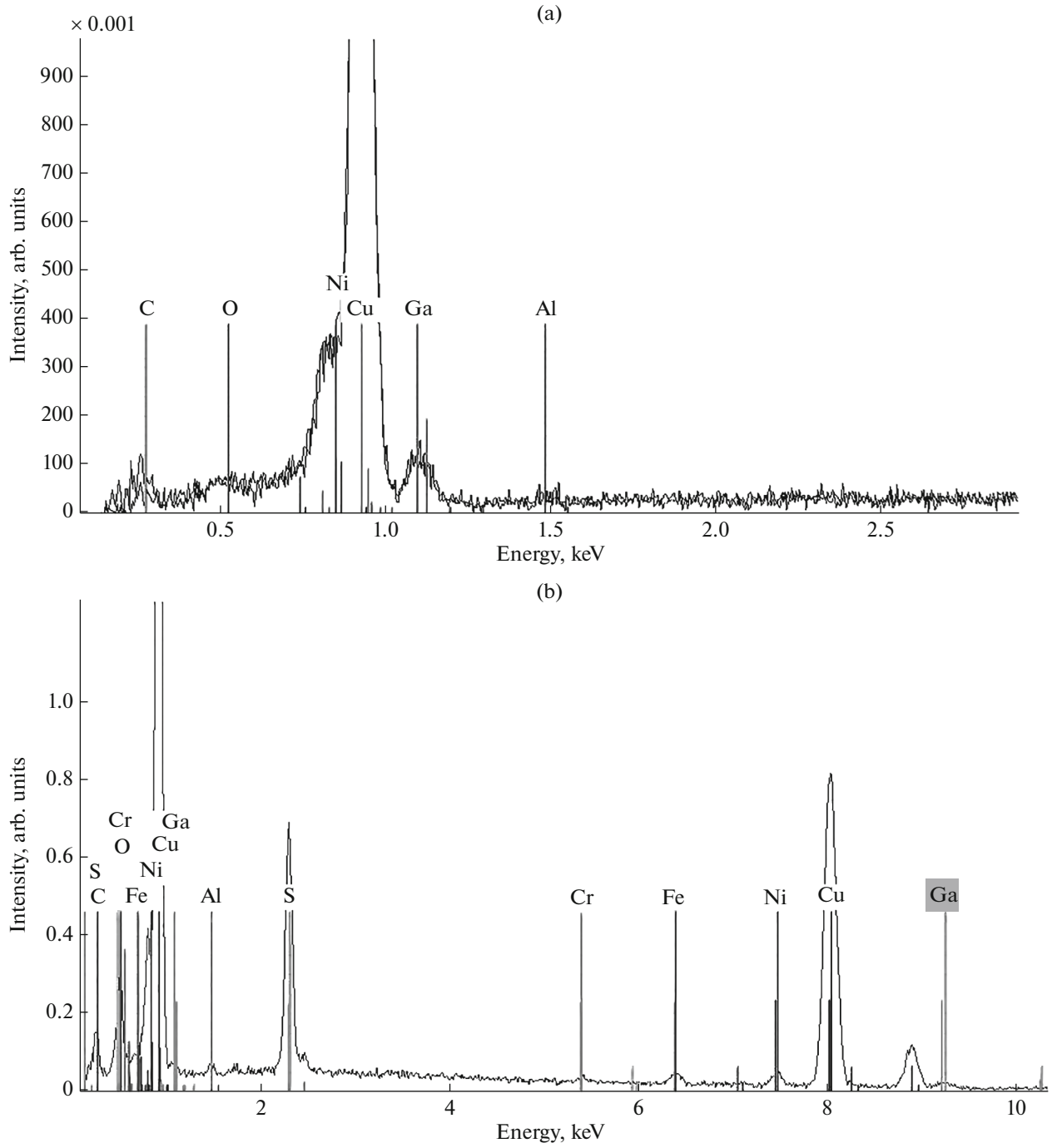

Fig. 10. X-ray spectra of elements in the irradiated surface layer of the Cu–4% Ni–10% Ga alloy: (a) experiment 1, sample 4 for two points in Fig. 9a (point 1 in the slip line and point 2 near the slip line); (b) experiment 2, sample 5: in a microparticle on the surface (Table 1).

parameters of the formation of such a structure are dependent on the mode of pulsed irradiation of the sample target and the conditions of subsequent directional solidification of the melted surface layer. In addition, doping of the copper–nickel binary alloy with a third element, gallium, and, supposedly, the dendritic structure of the alloy in the initial state noticeably influence the formation of the considered structure.

In the surface layer of each of the studied alloys upon irradiation with flows of deuterium plasma and deuterium ions under action of thermal stresses, plastic deformation proceeds by the slip over the planes of densest packing {111} typical of fcc materials.

The results of this work show that the ductile Cu–Ni and Cu–Ni–Ga copper alloys and also the Cu–10% Ga alloy, studied before [19], demonstrate a high crack resistance to the action of high-power pulsed radiation–thermal loads of nanosecond pulse duration generated in the Plasma Focus PF-1000 installation in comparison to refractory W, Mo, and V.

FUNDING

This work was performed in the framework of task no. 075-00947-20-00.

CONFLICT OF INTEREST

The authors declare that they have no conflicts of interest.

REFERENCES

1. V. A. Gribkov, F. I. Grigor'ev, B. A. Kalin, V. L. and Yakushin, *Advanced Radiation-Beam Technologies for Material Processing* (Kruglyi God, Moscow, 2001) [in Russian].
2. I. E. Garkusha, A. V. Burdakov, I. A. Ivanov, E. P. Kruglyakov, K. N. Kuklin, I. S. Landman, V. A. Makhlaj, S. V. Polosatkin, A. A. Shoshin, V. I. Tereshin, and N. N. Aksenov, Probl. At. Sci. Technol., Ser.: Plasma Phys. **14** (6), 58 (2008).
3. V. A. Gribkov, V. N. Pimenov, L. I. Ivanov, E. V. Dyomina, S. A. Maslyaev, R. Miklaszewski, M. Scholz, U. E. Ugaste, A. V. Doubrovsky, F. Mezzetti, V. C. Kulikauskas, and V. V. Zatekin, J. Phys. D: Appl. Phys. **36**, 1817 (2003).
4. P. N. Maier and A. E. Maier, Vestn. Chelyabinsk. Gos. Univ. Ser. Fiz. **11** (35), 41 (2011).
5. V. S. Kovivchak, T. V. Panova, V. I. Blinov, and R. B. Burlakov, Poverkhn.: Rentgenovskie, Sinkhrotronnye Neitr. Issled., No. 4, 69 (2006).
6. A. D. Pogrebnyak and Yu. N. Tyurin, Phys.—Usp. **48**, 487 (2005).
7. V. I. Tereshin, I. E. Garkusha, and V. V. Chebotarev, "Modification of surface layers of solids by powerful pulsed plasma flows. Radiation plasmodynamics," in *Encyclopedia of Low-Temperature Plasma*, Ed. by V. E. Fortov (Nauka, Moscow, 2007), Vol. 9, p. 442.
8. Z. G. Li, J. L. He, T. Matsumoto, T. Mori, S. Miyake, Y. Muramatsu, Surf. Coat. Technol. **173–174**, 1140 (2003).
9. R. Betti and O. A. Hurricane, Nat. Phys. **12**, 435 (2016). https://doi.org/10.1038/nphys3736
10. V. Ya. Bayankin, M. I. Guseva, D. I. Tetel'baum, and F. Z. Gil'mutdinov, Poverkhn.: Rentgenovskie, Sinkhrotronnye Neitr. Issled., No. 5, 77 (2005).
11. A. A. Novoselov, A. A. Shushkov, V. Ya. Bayankin, and A. V. Vakhrushev, Khim. Fiz. Mezoskopiya **14**, 609 (2012).
12. A. A. Novoselov, V. Ya. Bayankin, D. O. Filatov, A. A. Smirnov, and D. I. Tetel'baum, Vestn. NNGU. Ser. Fiz. Tverd. Tela, No. 2, 12 (2013).
13. M. V. Zhidkov, A. E. Ligachev, Yu. R. Kolobov, G. V. Potemkin, and G. E. Remnev, Izv. VUZov, Poroshk. Metall. Funkts. Pokrytiya, No. 4, 82 (2018). https://doi.org/10.17073/1997-308X-2018-4-82-91
14. A. V. Zhikharev, V. Ya. Bayankin, I. N. Klimova, S. G. Bystrov, A. Yu. Drozdov, and E. V. Kharanzhevskii, Phys. Solid State **57**, 845 (2015).
15. V. I. Mazhukin, A. V. Mazhukin, M. M. Demin, and A. V. Shapranov, Opt. Zh. **78** (8), 29 (2011).
16. I. V. Khomskaya, V. I. Zel'dovich, N. Yu. Frolova, and A. E. Kheifets, Bull. Russ. Acad. Sci.: Phys. **74**, 1546 (2010).
17. I. V. Khomskaya, Perspekt. Mater., No. 12, 551 (2011).
18. S. V. Razorenov and G. V. Garkushin, Tech. Phys. **60**, 1021 (2015).
19. I. V. Borovitskaya, V. A. Gribkov, A. S. Demin, N. A. Epifanov, S. V. Latyshev, S. A. Maslyaev, E. V. Morozov, V. N. Pimenov, I. P. Sasinovskaya, G. G. Bondarenko, A. I. Gaidar, and M. Scholz, Perspekt. Mater., No. 5, 23 (2020). https://doi.org/10.30791/1028-978X-2020-5-23-37
20. N. B. Volkov, A. E. Maier, and A. P. Yalovets, Tech. Phys. **47**, 968 (2002).
21. X. P. Zhu, M. K. Lei, Z. H. Dong, and S. M. Miao, Surf. Coat. Technol. **173**, 105 (2003). https://doi.org/10.1016/S0257-8972(03)00321-9
22. V. S. Kovivchak, T. V. Panova, and K. A. Mikhailov, J. Surf. Invest.: X-ray, Synchrotron Neutron Tech. **6**, 64 (2012).
23. G. G. Bondarenko, *Radiation Physics, Structure, and Strength of Solids* (BINOM. Laboratoriya Znanii, Moscow, 2016) [in Russian].
24. V. A. Gribkov, M. Paduch, E. Zielinska, A. S. Demin, E. V. Demina, E. E. Kazilin, S. V. Latyshev, S. A. Maslyaev, E. V. Morozov, and V. N. Pimenov, Radiat. Phys. Chem. **150**, 20 (2018).
25. I. V. Borovitskaya, V. N. Pimenov, V. A. Gribkov, M. Paduch, G. G. Bondarenko, A. I. Gaidar, V. V. Paramonova, and E. V. Morozov, Russ. Metall. (Eng. Transl.) **2017**, 928 (2017).
26. A. S. Demin, S. A. Maslyaev, V. N. Pimenov, V. A. Gribkov, E. V. Demina, S. V. Latyshev, M. M. Lyakhovitskii, I. P. Sasinovskaya, G. G. Bondarenko, A. I. Gaidar, and M. Paduch, Inorg. Mater.: Appl. Res. **8**, 412 (2017).
27. *Physical Metallurgy*, Ed. by R. W. Cahn and P. Haasen, 3rd ed. (North-Holland, Amsterdam, 1983; Metallurgiya, Moscow, 1987), Vol. 2.
28. N. D. Nyashina and P. V. Trusov, Vestn. Perm. Gos. Tekh. Univ. Mat. Model. Sist. Protsess., No. 6, 66 (1998).
29. V. A. Timofeeva, *Crystal Growth from Solution–Melt* (Nauka, Moscow, 1978) [in Russian].
30. A. G. Poskakalov, N. S. Klimov, Yu. M. Gasparyan, O. V. Ogorodnikova, and V. S. Efimov, Vopr. At. Nauki Tekh., Ser.: Termoyad. Sint. **41**, 23 (2018).
31. A. N. Ladygin and V. Ya. Sverdlov, Vopr. At. Nauki Tekh., Ser.: Fiz. Radiats. Povrezhdenii Radiats. Materialoved., No. 3, 132 (2004).
32. V. M. Azhazha, V. Ya. Sverdlov, A. A. Kondratov, A. V. Boguslaev, and V. V. Klochikhin, Vestn. Khar'kov. Univ., No 781, 73 (2007).
33. R. W. K. Honeycombe, *The Plastic Deformation of Metals* (Edward Arnold, London, 1968; Mir, Moscow, 1972).

Translated by Yu. Ryzhkov